TECHNICAL MEMORANDUMS

NATIONAL ADVISORY COMMITTEE FOR AERONAUTICS

No. 1021

PREDICTION OF DOWNWASH AND DYNAMIC PRESSURE AT

THE TAIL FROM FREE-FLIGHT MEASUREMENTS

By E. Eujen

Washington
July 1942

NATIONAL ADVISORY COMMITTEE FOR AERONAUTICS

TECHNICAL MEMORANDUM NO. 1021

PREDICTION OF DOWNWASH AND DYNAMIC PRESSURE AT

THE TAIL FROM FREE-FLIGHT MEASUREMENTS*

By E. Eujen

SUMMARY

The present measurements form a continuation of ear-
lier flight tests published in a previous report (refer-
ence 1) for predicting the downwash at the tail of an
airplane. The method makes use of the tail itself as
integrating contact surface to the extent that, beginning
from the measurement of the self-alinement of the elevator,
the mean downwash angle and dynamic pressure at the tail
are determined. The results are satisfactory, provided
certain assumptions are fulfilled. The instrumental
accuracy is considerably improved if the elevator is
completely separate from the controls during the tests,
because the effect of friction on the self-alinement of
the elevator is then reduced to a minimum and a finer
elevator weight balance is rendered possible. The struc-
tural design of the push-rod uncoupling mechanism is
described.

The knowledge of the flow phenomena at the tail is
of great importance for the precalculation of the longi-
tudinal stability of a projected type of aircraft. For
the case of power-on flight, however, the only information
available, up to now, is almost exclusively restricted
to an appraisal of experimental research. For this reason
the investigations on this subject are to be continued.

I. INTRODUCTION

In a previous report (reference 1) a flight test
method was described for predicting downwash and dynamic

pressure on the tail of an airplane. The two aeromechan-
ically important influence quantities α_w and q_H/q
were obtained as average value across the tail span by
measurement of the self-alinement of the elevator. Since
then, longitudinal stability investigations with free
elevator, afforded an opportunity for a further try-out
of the test method. Aside from that, the test data form
a contribution to the problem of wake characteristics on
the tail, since the elucidation of this question depends
the same as ever largely upon the statistical analysis
of suitable experimental material.

II. TESTING PROCEDURE

The downwash recording method is based on the set-
ting of a completely weight-balanced free elevator inde-
pendent of the magnitude of the air-stream velocity, on
the assumption that the tail consists of geometrically
similar profile sections. The mean angle of attack of
the tail α_H then follows from the elevator angle η_R
that is to be measured at

$$c_r = \left[\frac{\partial \, c_r}{\partial \, \alpha_H}\right]_{\eta_R} \alpha_H + \left[\frac{\partial \, c_r}{\partial \, \eta_R}\right]_{\alpha_H} \eta_R = 0 \quad * \tag{1}$$

For η_R and α_H in the region of steady flow the quotient

$$\frac{\partial \, c_r / \partial \, \eta_R}{\partial \, c_r / \partial \, \alpha_H}$$

is a constant essentially defined by the ratio of elevator
chord to tail chord. It can be measured direct on aircraft
with adjustable stabilizer (on ground or in flight) in a
flight test, by determining the change in elevator angle

---

*The elevator angle is indicated with η_R to differentiate
it from the stabilizer setting angle η_D relative to the
fuselage axis. For the rest the symbols follow the stand-
ard DIN L 100.

for a predetermined stabilizer setting (that is, α_H change). But it must not be accompanied by a change in the flight attitude itself and consequently in the flow at the tail - which can be accomplished by equalization of the action of the stabilizer setting with corresponding displacement of the center of gravity of the airplane. A further assumption of possible importance is that the reaction of the stabilizer setting on the wing lift and hence on the downwash distribution at the tail itself as well as the effect of the change in height position of the stabilizer mass due to the setting, remains small. It affords

$$\left[\frac{\Delta \eta_D}{\Delta \eta_R}\right]_{\alpha,\lambda \,=\, \text{const}} = \left[\frac{\Delta \alpha_H}{\Delta \eta_R}\right]_{\alpha,\lambda \,=\, \text{const}} = -\frac{\partial c_r / \partial \eta_R}{\partial c_r / \partial \alpha_H} \qquad (2)$$

This quantity has a value independent of the flight attitude as tail constant at constant elevator moment (inclusive of the special case $M_r = 0$) for a tail with geometrically similar profile sections across the span. If in any manner a given moment about the elevator axis is produced, the elevator setting is then not only dependent upon the angle of attack but also on the size of the dynamic pressure at the tail. The tail hereby assumes again the flight mechanically effective average value from the ordinarily very uneven distribution of dynamic pressure across the span.

Helmbold (reference 2) calls this average value the efficiency factor of the tail. With the mean angle α_H known from the previous downwash measurement for a specified flight attitude, while η_R is to be measured, the equilibrium of the moments about the elevator hinge at a control force moment M_{st} gives

$$\frac{q_H}{q} \frac{\partial c_r}{\partial \alpha_H} F_H \, l_H = -\frac{M_{st}}{\left(\alpha_H + \dfrac{\partial c_r / \partial \eta_R}{\partial c_r / \partial \alpha_H}\right) q} \qquad (3)$$

where the average dynamic pressure is expressed by the ratio q_H/q multiplied by the tail constants

$$\frac{\partial c_r}{\partial \alpha_H} F_H \, l_H = K$$

This factor K is not directly determinable by flight measurements. But in order still to be able to indicate the absolute value of the dynamic-pressure ratio in full-throttle flight, a certain assumption (that is, $q_H/q = 1$) must be made for the value q_H/q of power-off flight.

The present measurements were made with the Messerschmitt Bf 108 type airplane (fig. 1), the principal data of which are as follows:

Gross weight $G = 1235$ kg

Wing area $F = 16.7$ m^2

Wing loading $G/F = 74$ kg/m^2

Wing span $b = 10.6$ m

Aspect ratio $\Lambda = \dfrac{b^2}{F} = 6.72$

Engine Power $N_0 = 240$ hp

Power loading $G/N_0 = 5.14$ kg/hp

Wing chord at root $l = 2.00$ m

Mean aerodynamic chord at distance $\dfrac{2b}{3\pi}$ $l_m = 1.685$ m
   from body center

Incidence of wing with respect to fuse- $\epsilon = 2^0$
   lage axis inside and outside

Airfoil section - inside   NACA 2416

Airfoil section - outside   NACA 2413

Test range of center-of-gravity posi- $x_s = 0.288$ to 0.505 l
   tions, referred to mean aerodynamic
   chord

Position of thrust axis relative to $z_p = 0.19$ l
   leading edge of profile at wing root

Position of plane of propeller before $x_p = 0.88$ l
   the leading edge of profile at wing
   root

Backward and height position of elevator
   relative to trailing edge of profile $x_H = 1.465\ l$
      at wing root $z_H = 0.5\ l$

Distance of center of pressure of tail
   ($l_H/4$) from leading edge of wing
      at root $r_H = 2.06\ l$

Elevator area $F_H = 2.73\ m^2$

Effective elevator span $b_H = 3.096\ m$

Effective aspect ratio of tail $\Lambda_H = \dfrac{b_H^2}{F_H} = 3.51$

Ratio of areas $\dfrac{F_H}{F} = 0.1635$

Chord ratio $\dfrac{l_r}{l_H} = 0.425$

Diameter of propeller $D = 2.31\ m$

     (More detailed data on the propeller are given in
a subsequent report.)

     In conformity with the assumptions of the test method
the external aerodynamic balance of the elevator was re-
moved and the tail, as far as possible (opening for the
rudder!),given a constant spanwise elevator chord to total
chord ratio (fig. 2). The elevator uncoupling mechanism
installed for the planned longitudinal-stability studies
with free elevator was largely instrumental in the success
of the measurements; first, because it enabled a fine
weight balance of the elevator about its hinge, second
it afforded a practically frictionless elevator balance.
The uncoupling of the elevator was placed in the elevator
push rod, as suggested in the previous report. The mech-
anism (fig 3) consists of two telescopic pieces and a
strong coil spring maintaining a positive connection when
coupled. The uncoupling of the elevator is accomplished
by a piston under 6 to 8 atmospheres air pressure, which
compresses the spring and frees a length of 22 millimeters
for the part of the push rod connected with the elevator-
operating lever.

     This length of 22 millimeters corresponds,in the
present case, to a free range of elevator angle of about 10°.

The end deflections are indicated, within the push rod
across two contacts actuated by a cam on the movable part
of the rod, in the pilot's seat. The elevator is not com-
pletely free from external forces, even in the uncoupled
condition, because the weight of the push rod itself pro-
duces a certain moment about the elevator hinge, depend-
ing upon the longitudinal inclination of the aircraft and
the elevator setting. However, the most unfavorable case
failed to disclose a measurable effect on the self-aline-
ment of the elevator according to an estimation.

Figure 4 shows the installation of the instruments
comprising two DVL duplex recorders for dynamic pressure,
static pressure, angle of attack, and rotative speed, also
a pendulum banking indicator. The elevator angle recorder
was in this instance a mechanical recorder with very long
cylinder; the transmission between elevator and stylus
was chosen so as to utilize as far as possible the total
record height of 16 centimeters for recording the eleva-
tor range in question (1 cm stylus travel $\approx$ 1° elevator
angle). The pitot static tube combined with a dual-orifice
nozzle for recording the angle of attack was mounted to
an arm extending beyond the trailing edge for instrumental
reasons (fig. 5). But the distance from the wing was not
so great that an influence on the test data by the circu-
lation about the wing tip could no longer be expected.
Hence the reading error had to be determined by calibration
of the pitot tube by means of total head tube and static
trailing pitot. Because of the incorrect reading the
pressure differences recorded by angular pitot could not
be used immediately for determining the angle of attack;
hence the conventional method involving path and longi-
tudinal inclination, with its inevitably greater inaccu-
racies, was resorted to.

A given moment was applied to the elevator hinge by
means of a lead weight placed on the elevator trailing edge.
But, since the elevator moment is not constant by this
arrangement but rather varies with the cosine of ($\delta + \eta_D + \eta_R$)
this fact must be reflected in the calculation of q_H/q K
according to equation 3.

For the rest the testing procedure was the same as
described in the previous report (reference 1).

III. RESULTS OF TESTS

The effect of the propeller rotating on the mean downwash and dynamic pressure at the tail was obtained by a comparison of the flight-test data for power on and power off. The original plan was to make the tests with feathering propeller rather than in power-off flight so as to obtain a better basis of comparison for the theoretically defined downwash values. But due to failure of the arrival of the necessary adjustable pitch propeller this had to be temporarily postponed. The automatic wing slots with which the Bf 108 is normally fitted, were blocked in the closed position.

The downwash angle at the tail for one of the operating conditions follows, on the one hand, from the evaluation of the measurement of the lift coefficient in relation to the angle of attack,* and on the other, from the relations between the self-alinement of the free elevator and the lift coefficient of the airplane determined at two constant stabilizer settings. Neither the drag coefficients nor the airplane polars are of themselves necessary for the appraisal; they are but a secondary result of the measurements and were merely included for the sake of completeness (figs. 8, 9). Despite the considerable scatter involving the evaluation of the time rate of change in barometric pressure, a certain amount of balance was still obtainable with a greater number of measurements. The scatter of the test points in power-off flight attending the plotting of the coefficient of advance against the lift coefficient (fig. 10) is due to the fact that, on one hand, every error in the rotative speed measurement reacts inversely proportional to the square of the speed when computing the coefficient of advance, and at the other, the engine in power-off attitude reacts more susceptibly to the state of the surrounding air. The angle of attack of the body axis α_L at the tail is obtained from the measurements with fully weight-balanced elevator by the foregoing method and from the definitions of the angles (fig. 13). It results in the curve, shown in figure 14. The difference $\alpha_F - \alpha_L$ is the desired downwash angle α_w plotted against the airplane angle of attack α_F in figure 15 for power on and power off.

---

*The angle of attack referred to fuselage axis at the wing is indicated with α_F to differentiate it from that of the fuselage axis at the tail α_L.

The theoretical downwash without wake effect is shown as dashed curve. For the prediction of these downwash angles the lift distribution of the wing was defined by the Multhopp method (reference 3) on the basis of the given structural data. The downwash angles themselves were secured by interpolation from the design charts contained in NACA Report No. 648. The conspicuous difference in absolute values observed in the comparison between the experimental downwash in power-off flight and the theoretical downwash is largely due to the fact that the determination of the geometric angles on the airplane (angle of setting of wing and stabilizer with respect to fuselage axis) is possible only with a limited degree of accuracy. The only essential factor for the stability contribution of the tail is the slope of the curves shown in figure 15 in form of the downwash factor

$$A_1 = \left[1 - \frac{d\alpha_w}{d\alpha_F} \right]$$

This amounts to $A_1 = 0.62$ in the designated theoretical case as against $A_1 = 0.65$ for the power-off flight test. The stabilizing effect of the tail is accordingly greater in power-off flight than the calculation manifests. But this difference is a mere 5 percent and likely to be due to a drop in wing lift distribution which might be caused by the effect of the rotating propeller and the fuselage.

The decrease in stabilizing effect of the tail in full-throttle flight is perceptible, although not as much as on the Klemm Kl 36 A (reference 1). The downwash factor in full-throttle flight for the Bf 108 amounts to $A_1 = 0.52$ in the middle portion of the curve and drops to $A_1 = 0.47$ ($\alpha_F = 10°$) at greater angles of attack. The tendency in power-off flight is the opposite.

Wool-tuft records during flight and observations indicated that the flow at the wing root is steady in full-throttle flight even at maximum lift coefficients (fig. 16). Separation phenomena rather appeared first at the flap trailing edge, while in power-off glide the flow separated first at the wing root at lifts above $c_a = 0.7$ (fig. 17), consistent with the incipient downward curvature of the downwash curve. In a peculiar manner this breakdown of flow is not reflected in the relationship of lift to angle of attack (fig. 7).

The control-force moment applied at the elevator for determining the dynamic pressure was 0.282 mkg ($\vartheta = \eta_D = \eta_R = 0$).

The values q_H/q K calculated from the measurements for two operating conditions disclosed the relationship with the airplane angle of attack α_F shown in figure 18. The prediction of the mean dynamic pressure ratio q_H/q for full throttle (dashed curve in fig. 18) was based upon the mean value q_H/q K $= -0.075$ of the power-off measurement. The variation of the curve indicates that the tail strays out of the stream with increasing angle of attack as reflected in the dynamic pressure data which after an initial rise drop again at greater angles of attack. The maximum value obtained was $q_H/q = 1.25$. From the plotting of efficiency factor q_H/q and tail angle $\alpha_H(\eta_D = 0)$ as function of α_F (fig. 19) the the tail quality factor (reference 5)

$$\frac{d(q_H/q \; \alpha_H)}{d\alpha_F}$$

can then be determined; it amounts to 0.635 in full-throttle flight.

The experimental results can be regarded as satisfactory in every respect. On this favorable result, the uncoupling of the elevator from the control shared very considerably, since the reduced friction caused only very little scatter of the test points compared to the approximate size of the differences in experimental elevator angle.

The independence of quotient

$$\frac{\Delta \, \eta_D}{\Delta \, \eta_R} = - \frac{\partial \, c_r/\partial\eta_R}{\partial \, c_r/\partial\alpha_H}$$

from the flight attitude, which forms an important assumption of the test method, prevails throughout the entire experimental flight range for the weight-balanced elevator. The obtained numerical value of

$$\frac{\partial \, c_r/\partial \, \eta_R}{\partial \, c_r/\partial \, \alpha_H} = 2.63$$

is in close agreement with model tests on tails with similar elevator chord ratios l_r/l_H. In the measurements for predicting the dynamic pressure at the tail, no constancy of value $\dfrac{\Delta \eta_D}{\Delta \eta_R}$ is to be expected, since the moment applied about the elevator axis varies with the longitudinal inclination of the airplane and with the tail angles. The discrepancies, however, are not very great.

Translation by J. Vanier,
National Advisory Committee
for Aeronautics.

REFERENCES

1. Eujen, E.: Flugmessungen über den Einfluss von Schraubenstrahl und Landeklappenanstellung auf Abwind und Staudruck am Höhenleitwerk. Luftfahrtforschung, Jan. 10, 1939, vol. 16, no. 1, pp. 38-46.

2. Helmbold, H.B.: Untersuchung über den Einfluss des Luftschraubenstrahls auf den Abwind und die Höhenleitwerkswirkung. Luftfahrtforschung, Jan. 20, 1938, vol. 15, no. 1-2, pp. 3-8.

3. Multhopp, Hans: Die Berechnung der Auftriebsverteilung von Tragflügeln. Luftfahrtforschung, April 6, 1938, vol. 15, no. 4, pp. 153-169.

4. Silverstein, Abe, and Katzoff, Samuel: Design Charts for Predicting Downwash Angles and Wake Characteristics behind Plain and Flapped Wings. Rep. No. 648, NACA, 1939.

5. Flügge-Lotz, I, and Küchemann, Dietrich: Zusammenfassender Bericht über Abwindmessungen ohne und mit Schraubenstrahl. Jahrb. 1938 der deutschen Luftfahrtforschung, pp. I 172-193.

Figure 2.— View of tail alterations.

Figure 5.— Pitot tube at wing tip.
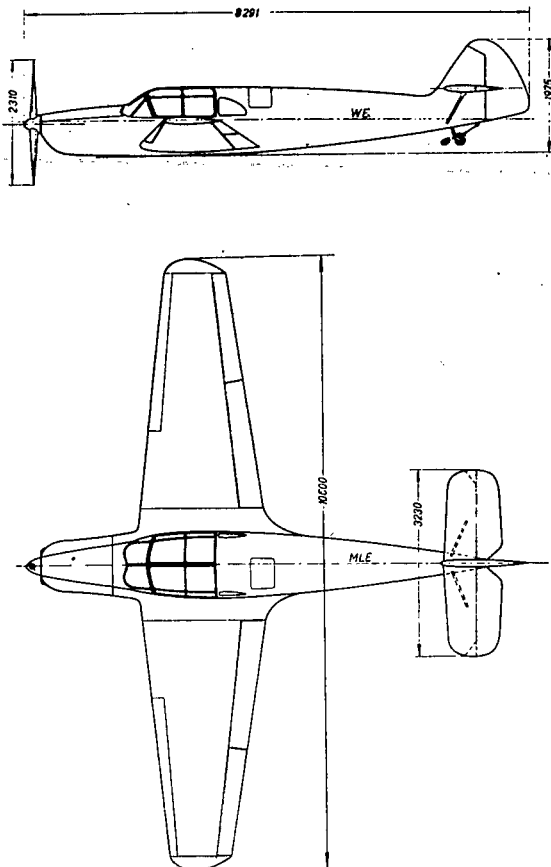
Figure 1.— Experimental airplane Bf 108.
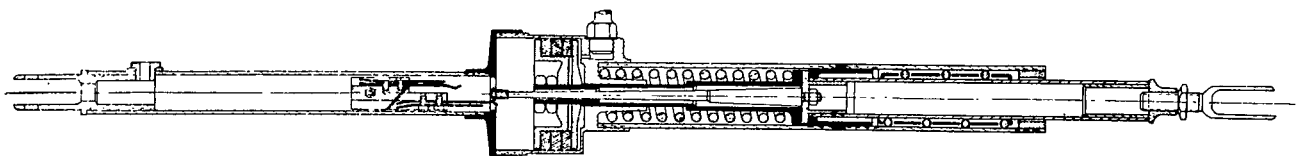
Figure 3.— Push rod uncoupling mechanism for elevator.

Figure 4.— View of test instruments in cockpit.
      (a) dual recorder, (b) banking recorder, (c) time making
mechanism, (d) compressed air flask for elevator uncoupling, (e)
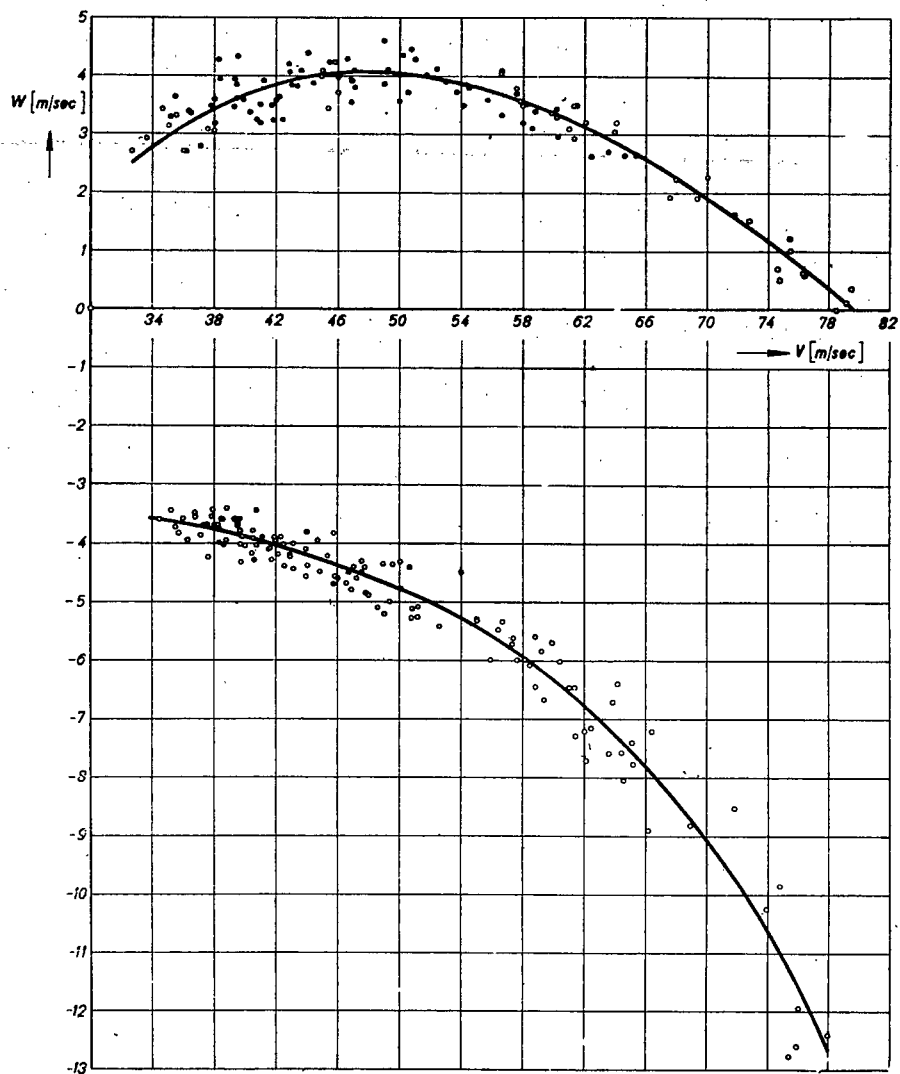operation of weight, (f) instrument switch.

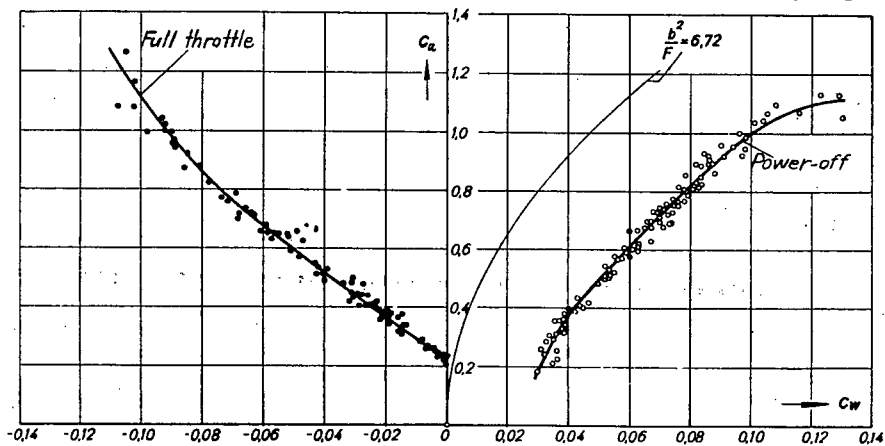Figure 6.— Rate of climb and sinking speed against flying speed.

Figure 9.— Airplane polars for full throttle and power-off flight.
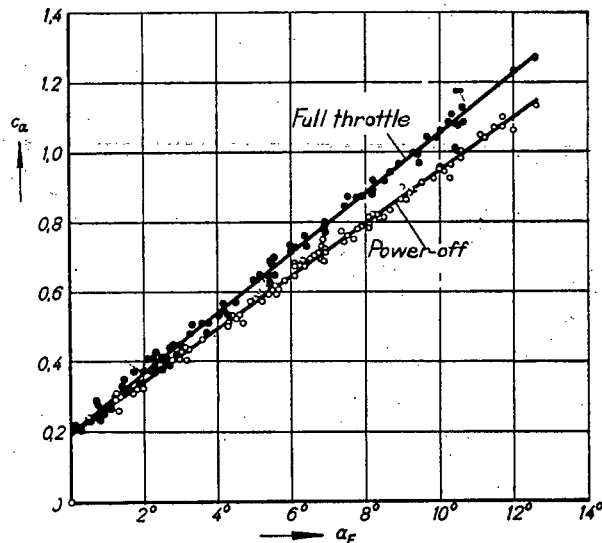
Figure 7.— Lift coefficient plotted against angle of attack of fuselage axis for power-off and full throttle flight.
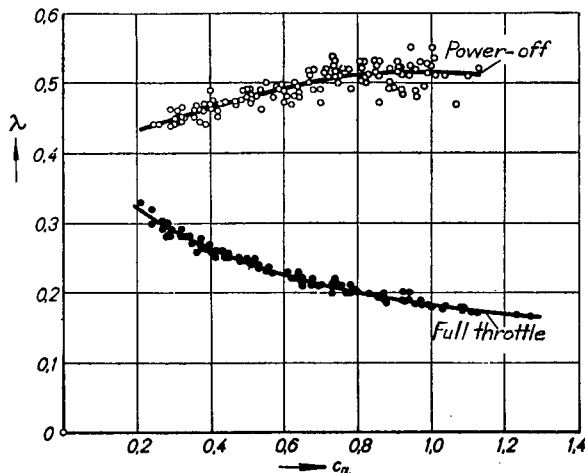
Figure 10.— Coefficient of advance against lift coefficient for full throttle and power-off flight.
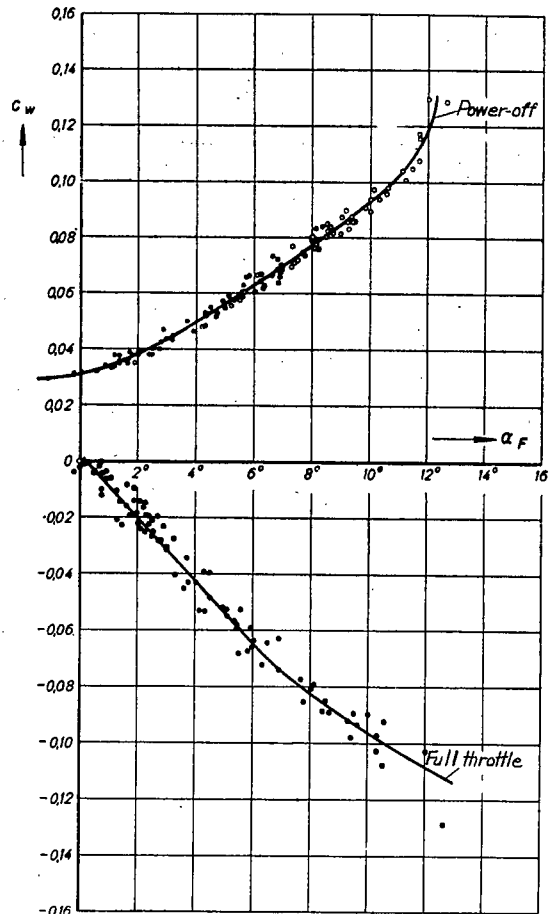
Figure 8.— Drag coefficient plotted against angle of attack of fuselage axis for full throttle and power-off flight.
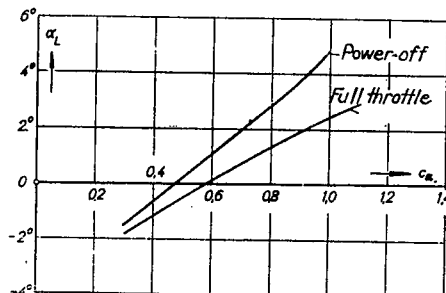
Figure 14.— Angle of attack of fuselage axis at tail against angle of attack of fuselage axis at wing.
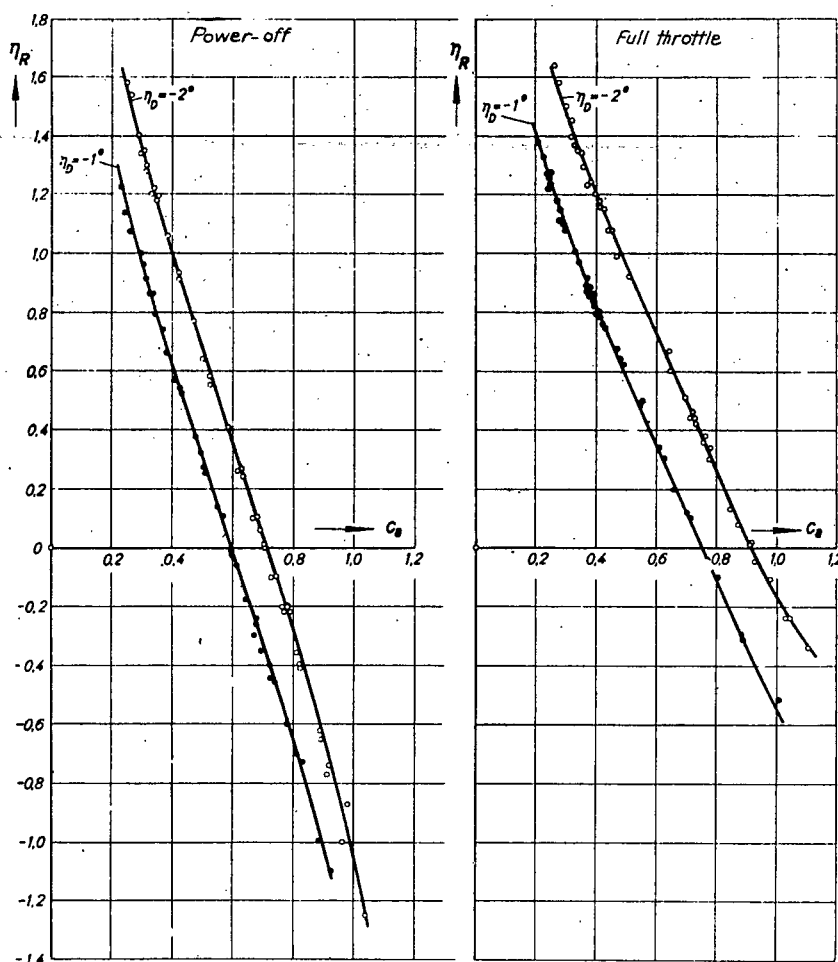
Figure 11.- Elevator angle against lift coefficient with weight-balanced elevator for full throttle and power-off flight.

$$\alpha_L = \alpha_H - \eta_D$$
$$\alpha_W = \alpha_F - \alpha_L$$
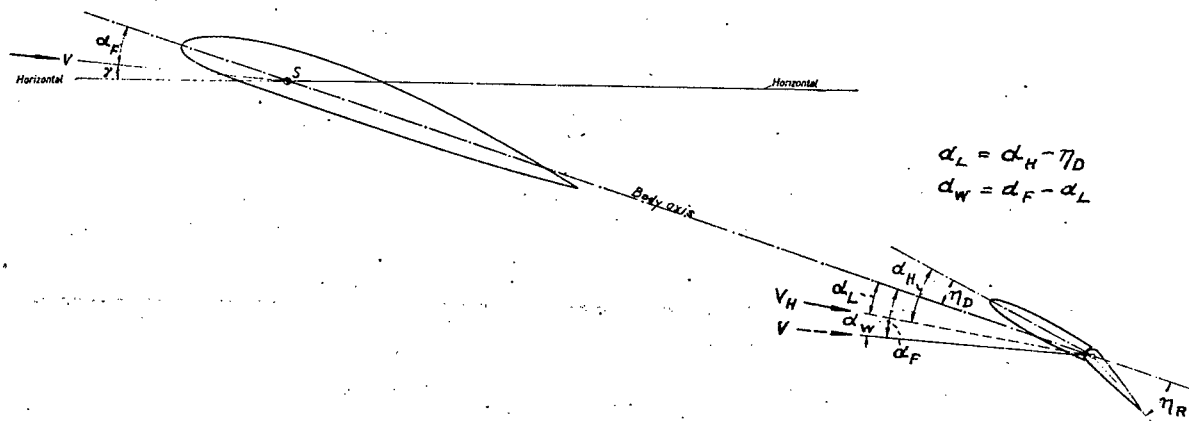
Figure 13.- Identification of angles.
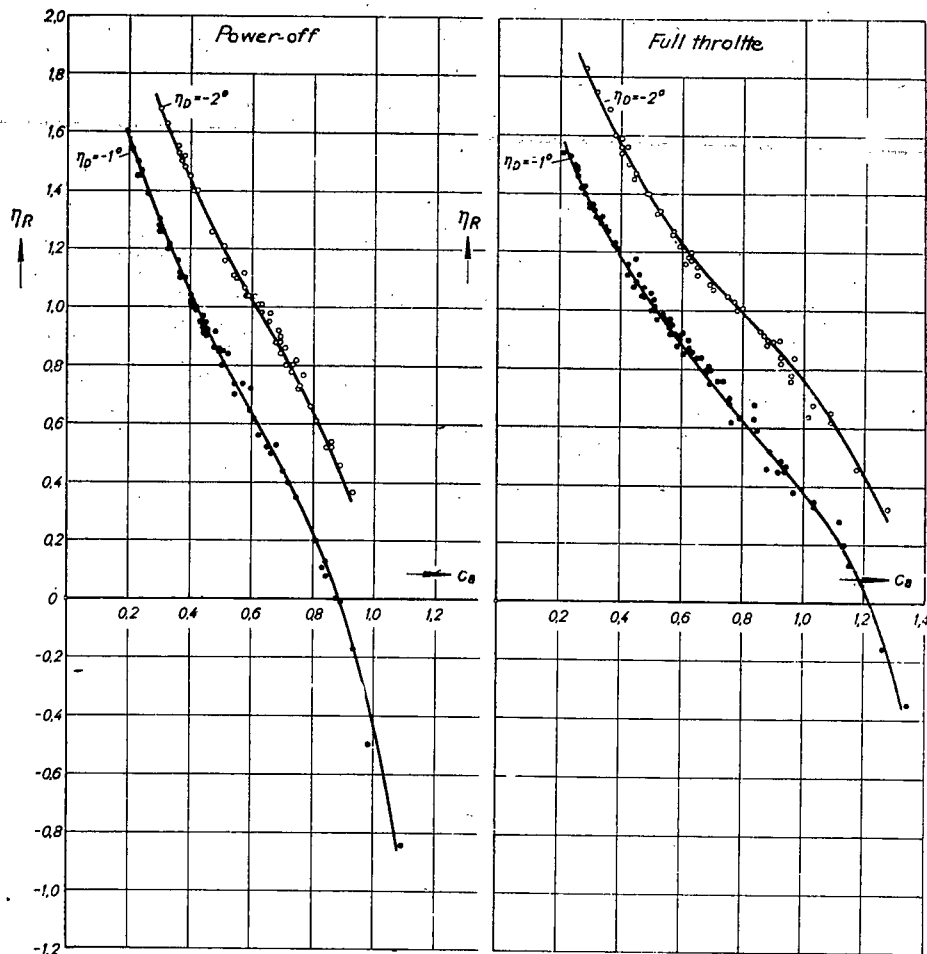
Figure 12.- Elevator angle against lift coefficient at control force
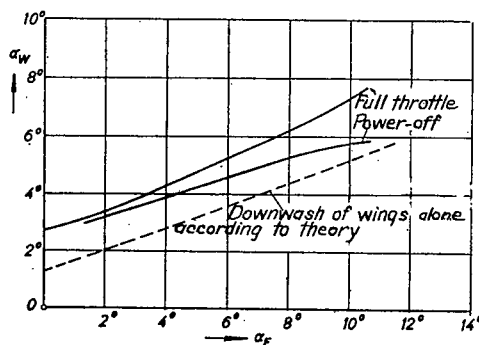moment M_{st} = 0.282 mkg for full throttle and power-off flight.

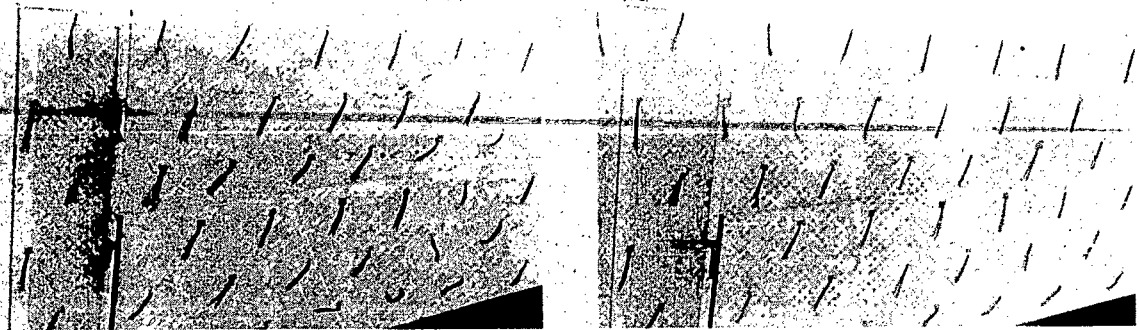Figure 15.- Downward angle at tail as function of α_F for full throttle and
power-off flight.

Figure 16.- Wool tuft record on inboard portion of wing at full throttle.
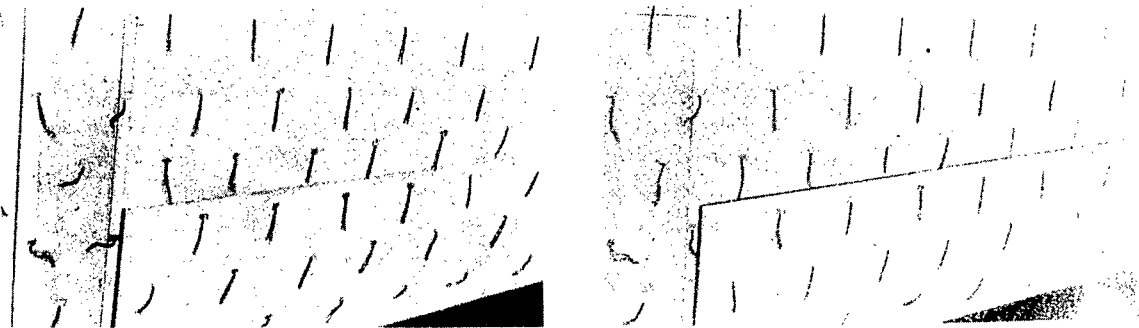(a) $c_a = 0.925$ $\alpha_F = 8.4^0$. (b) $c_a = 1.275$ $\alpha_F = 12.3^0$.

Figure 17.- Wool tuft record on inboard portion
of wing at power-off flight.
(a) $c_a = 0.74$ $\alpha_F = 7.2^0$. (b) $c_a = 0.925$ $\alpha_F = 9.7^0$. $\frac{q_H}{q} \cdot \alpha_H$

Figure 19.- Diagram
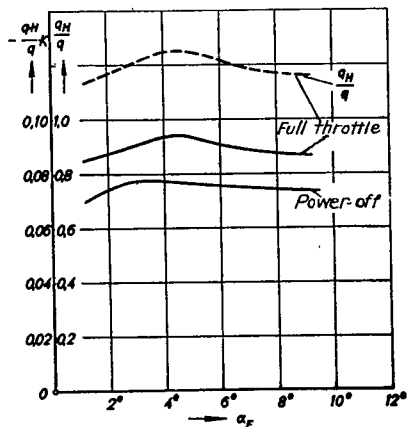for
defining the tail
efficiency.

Figure 18.- Dynamic pressure at tail
against angle of attack
of airplane.